

# JGR Atmospheres

## RESEARCH ARTICLE

10.1029/2019JD031243

### Key Points:

- The two rainy seasons have gotten longer and wetter, with significant increases in duration and rainfall total for the first rains
- Rainfall increased in all seasons, except DJF, throughout the region, and southwestern Uganda had the largest increase in annual rainfall
- Congo westerlies contribute substantially to rainfall, especially during JJA and SON, but were not responsible for the wetting trends

### Supporting Information:

- Supporting Information S1

### Correspondence to:

J. E. Diem,  
jdiem@gsu.edu

### Citation:

Diem, J. E., Sung, H. S., Konecky, B. L., Palace, M. W., Salerno, J., & Hartter, J. (2019). Rainfall characteristics and trends—and the role of Congo westerlies—in the western Uganda transition zone of equatorial Africa from 1983 to 2017. *Journal of Geophysical Research: Atmospheres*, 124, 10,712–10,729. <https://doi.org/10.1029/2019JD031243>

Received 26 JUN 2019

Accepted 11 SEP 2019

Accepted article online 15 SEP 2019

Published online 24 OCT 2019

### Author Contributions:

**Conceptualization:** Jeremy E. Diem, Hae Seung Sung, Bronwen L. Konecky

**Data curation:** Jeremy E. Diem

**Formal analysis:** Jeremy E. Diem, Hae Seung Sung, Michael W. Palace

**Funding acquisition:** Jeremy E. Diem

**Investigation:** Jeremy E. Diem

**Methodology:** Jeremy E. Diem, Hae Seung Sung

**Project administration:** Jeremy E. Diem

**Resources:** Jeremy E. Diem

**Software:** Jeremy E. Diem, Hae Seung Sung, Michael W. Palace

**Supervision:** Jeremy E. Diem

**Writing - original draft:** Jeremy E. Diem, Hae Seung Sung

**Writing - review & editing:** Jeremy E. Diem, Hae Seung Sung, Bronwen L. Konecky, Michael W. Palace, Jonathan Salerno, Joel Hartter

## Rainfall Characteristics and Trends—and the Role of Congo Westerlies—in the Western Uganda Transition Zone of Equatorial Africa From 1983 to 2017

Jeremy E. Diem<sup>1</sup> , Hae Seung Sung<sup>1</sup> , Bronwen L. Konecky<sup>2</sup> , Michael W. Palace<sup>3</sup>, Jonathan Salerno<sup>4</sup>, and Joel Hartter<sup>5</sup>

<sup>1</sup>Department of Geosciences, Georgia State University, Atlanta, GA, USA, <sup>2</sup>Department of Earth and Planetary Sciences, Washington University, St. Louis, MO, USA, <sup>3</sup>Department of Earth Sciences, University of New Hampshire, Durham, NH, USA, <sup>4</sup>Human Dimensions of Natural Resources, Colorado State University, Fort Collins, CO, USA, <sup>5</sup>Environmental Studies Program, University of Colorado Boulder, Boulder, CO, USA

**Abstract** While long-term rainfall trends and related atmospheric dynamics have been researched over the past several decades across equatorial Africa, little is known about rainfall in western Uganda, a transition zone in the middle of the continent. Using satellite-derived rainfall and reanalysis data from 1983 to 2017, this study examines atmospheric characteristics of seasons and multidecadal trends in rainfall. Most of the region has a biannual rainfall regime (i.e., the first rains within March–May and the second rains during August–November). Ascending (descending) air and increased (decreased) specific humidity are observed over western Uganda during the rainy (dry) seasons. Southeasterly air-parcel back trajectories are common throughout western Uganda at all times except for the first dry season (i.e., December–February). For all seasons, wet days in western Uganda are characterized by increases in ascending air and specific humidity in addition to westerly flow anomalies. Wet days in most seasons also have a disproportionately high frequency of westerly back trajectories extending over the Congo Basin. These Congo westerlies are associated with more vertical ascent and a more humid middle troposphere compared to the other trajectories. Rainy seasons, especially the first rains, have gotten longer and wetter throughout western Uganda. The duration of the first rains increased by about 1 month over the 35 years; in turn, the rainfall total increased by approximately 70%. Rainfall also has increased for climatological seasons, with the exception being December–February. Increases in middle-troposphere specific humidity and vertical ascent over time provide support for the wetting trends derived from the satellite-derived rainfall data.

## 1. Introduction

Rural communities in equatorial Africa rely predominantly on rainfed agriculture and so are intimately connected to seasonal rainfall patterns (Cooper et al., 2008; Zougmore et al., 2018). Therefore, developing a better understanding of the controls and variability of seasonal rainfall in equatorial Africa is important for improving food security in the region. In general, rainfall is tied to the movement of the tropical rainbelt and the Congo air boundary (CAB). The rainbelt is located over equatorial Africa mostly during the equinoctial months; therefore, the rainy seasons coincide with boreal spring (i.e., March–May, MAM) and fall (i.e., September–November, SON; Dezfuli & Nicholson, 2013; Nicholson, 1996; Nicholson & Dezfuli, 2013; Washington et al., 2013). The CAB is a confluence zone of unstable air from the Congo Basin and more stable air from the Indian Ocean (Costa et al., 2014; Dezfuli, 2017; Levin et al., 2009; Nicholson, 2000).

Rainfall varies greatly between central equatorial Africa (CEA) and eastern equatorial Africa (EEA). CEA exists almost entirely within the Democratic Republic of Congo and thus contains a large portion of the Congo rainforest (Todd & Washington, 2004), and EEA includes eastern Uganda, Kenya, Tanzania, and Somalia (Monaghan et al., 2012). CEA receives more annual rainfall than EEA, and much of CEA is considered to have a humid regime (i.e., no dry season; Liebmann et al., 2012; Dunning et al., 2016). But CEA does tend to have decreased rainfall during boreal winter (i.e., December–February, DJF) and summer (June–August, JJA; Dezfuli, 2017; Washington et al., 2013). Most of EEA has a biannual rainfall regime (i.e., two rainy seasons), with more rainfall occurring during the first rainy season (i.e., the long rains), which occur during MAM, compared to the second rainy season (i.e., the short rains), which occur from October–December (Camberlin et al., 2009; Liebmann et al., 2012). CEA has the opposite situation: SON rainfall is greater than MAM rainfall (Creese & Washington, 2018).

Both CEA and western EEA tend to receive more rainfall when there are low-level westerlies. The Congo westerlies are a major feature of CEA: They transport moisture from the Atlantic Ocean and thus contribute to the development of the tropical rainbelt and CAB (Grist & Nicholson, 2001; Nicholson & Grist, 2003), and they are associated with wet days in the region (Dezfuli & Nicholson, 2013; Nicholson & Dezfuli, 2013; Nicholson & Grist, 2003). The westerlies also have a large influence on rainfall in western EEA: Wet days and wet seasons in the western portion of EEA such as Uganda, western Kenya, and southwestern Ethiopia are associated with low-level, westerly wind anomalies, which contain the moisture from the Congo Basin (Camberlin, 1997; Camberlin & Philippon, 2002; Pohl & Camberlin, 2006a, 2006b; Williams et al., 2012). Mountainous terrain in western Kenya prevents much Congo moisture from reaching eastern EEA (i.e., eastern Kenya, northeastern Tanzania, and Somalia), which is much drier than the western region (Nicholson, 1996).

EEA has undergone a long-rains drying trend. Rainfall in months coinciding with the long rains has decreased significantly over the past several decades (Funk et al., 2008; Liebmann et al., 2014; Lyon & DeWitt, 2012; Yang et al., 2014). The drying trend has been hypothesized to have been caused by increases in central Indian Ocean sea surface temperatures, which, in turn, caused a westward extension of the Walker circulation and thus more descending air over EEA (Funk et al., 2008; Williams & Funk, 2011).

CEA also may have experienced a drying trend, but there is much less confidence in rainfall trends in the region compared to EEA. A large reduction in the number of rain gauges in CEA over the past several decades (Nicholson et al., 2019; Washington et al., 2013) has made the use of satellite-based estimates vital for assessing rainfall trends (Diem et al., 2019). Results from satellite products that rely heavily on contemporaneous gauge data show decreasing trends for the following: April–June rainfall from 1979 to 2014 (Hua et al., 2016); annual rainfall from 1979 to 2004 (Yin & Gruber, 2010); and annual rainfall from 1983 to 2010 over large parts of CEA (Maidment et al., 2015). However, given that the ground measurements are severely lacking in CEA (Washington et al., 2013), satellite-based trends in this region from those products referenced above, which include African Rainfall Climatology Version 2 (Novella & Thiaw, 2013), might be artificial (Maidment et al., 2015). Data from The TAMSAT African Rainfall Climatology And Timeseries (TARCAT; Maidment et al., 2014), which is a satellite-based product that does not rely on contemporaneous gauge data, have shown that annual rainfall may have increased from 1983 to 2008 (Maidment et al., 2015).

Western Uganda has been considered the transition zone between CEA and EEA (Figure 1), and there is debate about whether rainfall has been increasing or decreasing in the region. Mean annual rainfall totals in this region are much higher than totals in EEA as a whole and slightly lower than totals in CEA (Diem et al., 2014). Despite western Uganda being commonly included as part of EEA, the rainy seasons in western Uganda are similar to those in CEA: The rainfall in MAM is less than that in SON; therefore, the first rains of the year are called the “short rains,” and second rains are called the “long rains” (Diem et al., 2017; Hartter et al., 2012). Similar to CEA, the number of rain gauges in western Uganda has not been consistent over time (Christy, 2013; Kizza et al., 2009). While results using African Rainfall Climatology Version 2 data show that annual rainfall may have decreased significantly in western Uganda during the past several decades (Diem et al., 2014; Ssentongo et al., 2018), after adjusting for drying biases in three satellite-based products, annual rainfall in western Uganda has been shown to have significantly increased from 1983 to 2016 (Diem et al., 2019). In addition, wetting trends in rainy seasons and drying trends in dry seasons were found using data from 1983 to 2016 and 1997–2016 from TARCAT data and Climate Hazards Group InfraRed Precipitation with Stations (CHIRPS; Funk et al., 2015), and farmers have been perceiving these changes (Salerno et al., 2019).

Since western Uganda has been greatly understudied, especially with respect to EEA, an examination of multidecadal trends in rainfall and related variables as well as an examination of atmospheric variables during rainy and dry seasons is needed for the region. The vast majority of households in western Uganda, which include over 6 million people (Stevens et al., 2015), practice rainfed small-scale agriculture; therefore, planting and harvesting cycles are timed with the onset and cessation of the rainy season for the major crops (Hartter et al., 2012). Although Salerno et al. (2019) examined multidecadal trends of rainfall by seasons in the region, only a few locales were studied. Diem et al. (2019) examined western Uganda as a whole but did not examine changes in rainy and dry seasons. In addition, western Uganda has been included—often as a small part of a domain—in rainfall and circulation studies with diverse geographic scales; examples

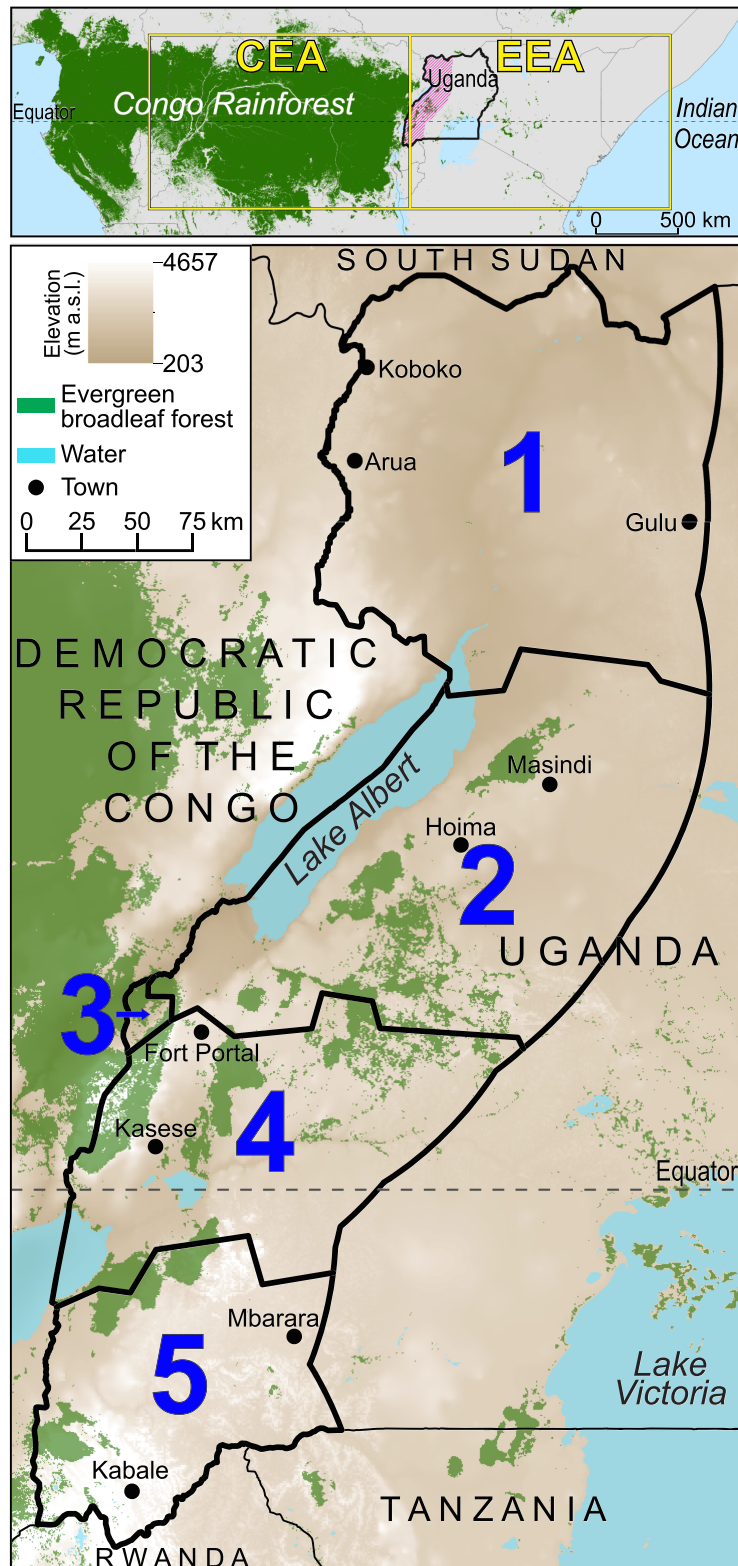


**Figure 1.** Location of western Uganda, which has been defined as a zone within 160 km of the Congo Basin (Diem et al., 2019), with respect to the Congo rainforest, central equatorial Africa (CEA), and eastern equatorial Africa (EEA). Land-cover information is derived from the Moderate Resolution Imaging Spectroradiometer land cover type product (MCD12Q1). The five rainfall regions within western Uganda also are shown, and the development and description of these regions are described in sections 3 and 4.

include Kenya and Uganda (Ongoma et al., 2018; Otieno & Anyah, 2013), eastern Africa (Nicholson, 2017), EEA (Gitau et al., 2018); the Greater Horn of Africa (Nicholson, 2014; Williams et al., 2012), and CEA or Congo Basin (Creese et al., 2019; Creese & Washington, 2018; Dezfuli & Nicholson, 2013; Hua et al., 2018, 2019; Nicholson & Dezfuli, 2013). Not only is it not known how rainy-season rainfall characteristics have changed over time within western Uganda, but it also is not known what atmospheric conditions lead to wet days and dry days within the rainy and dry seasons. Consequently, the overarching goal of this research is to greatly improve the understanding of seasonal rainfall characteristics and trends in western Uganda, which as noted before is a region with greatly conflicting information regarding trends in rainfall, with some studies finding drying trends (Diem et al., 2014; Ssentongo et al., 2018) and other studies finding wetting trends (Diem et al., 2019; Salerno et al., 2019). The three objectives are to examine the following: (1) atmospheric characteristics of seasons and wet days within seasons; (2) the influence of Congo westerlies on rainfall; and (3) multidecadal trends in rainfall.

## 2. Data and Methods

### 2.1. Precipitation

Daily precipitation data from two satellite-based rainfall data sets, CHIRPS and TAMSAT-2 (also known as TARCAT in previous papers), were used to examine rainfall variability from 1983 to 2017. CHIRPS and TAMSAT-2 begin in 1981 and 1983, respectively, and have spatial resolutions of  $0.05^\circ$  and  $0.0375^\circ$ , respectively. Although the latest version (v3.0) of TAMSAT does not underestimate rainfall totals like TAMSAT-2 does (Maidment et al., 2017), TAMSAT-3 was not used in this study, because rigorous analyses of the temporal stability of TAMSAT-3 in western Uganda have not been conducted. CHIRPS is a serially complete database, while 2.2% of the TAMSAT-2 daily totals were either missing or deemed erroneous (i.e., series of days with identical nonzero values) by the authors of this paper. Based on results from change-point analyses specific to western Uganda, CHIRPS data have been found to have a drying bias than begins in 1989 and to have suppressed estimates during 2007–2010, while TAMSAT v2.0 may be considered to be homogeneous and thus not have any significant change points (Diem et al., 2019). Therefore, daily TAMSAT v2.0 estimates were not adjusted, but daily CHIRPS estimates from January 1983 to July 1989 were multiplied by 0.9353 and daily estimates from March 2007 through April 2010 were multiplied by 1.1899 (Diem et al., 2019).

### 2.2. Rainfall Regionalization

Since rainfall patterns have been shown to vary substantially within western Uganda (Diem et al., 2019), the study domain was divided into rainfall regions (i.e., regions with homogeneous rainfall variability). CHIRPS was used for the regionalization, because it is more accurate than TAMSAT-2 at estimating rainfall totals across western Uganda (Diem et al., 2019). Regionalization was performed via hierarchical cluster analysis (Badr et al., 2015) of monthly mean rainfall estimates from CHIRPS data from 1983 to 2017. The clustering was iterative, and final set of regions was selected based on a combination of maximizing rainfall differences among the regions and a logical physical partitioning of western Uganda.

### 2.3. Rainy Seasons and Dry Seasons

Rainy and dry seasons for each year were defined using both CHIRPS and TAMSAT-2 data, using a modified version of the methodology in Dunning et al. (2016). Since TAMSAT-2 had 278 days with invalid rainfall values, the rainfall totals for those days were replaced with the mean value for that particular day of the year. The start and end of the climatological water seasons (1983–2017) were defined using the cumulative differences over the course of a climatological year between the climatological mean rainfall for the day of a year minus the mean daily rainfall total derived from all days. The procedure was repeated for each year using only rainfall totals and the mean daily rainfall total for that year, with all starting and ending dates constrained to occur within 30 days of the climatological starting and ending days. The values were then subsequently adjusted—if necessary—by examining the cumulative-difference plots for each year.

Wet days and dry days were identified within each rainy season using both rainfall products. Since not all days in a rainy season have rainfall, a day that had one  $\geq 1$  mm of rain was classified as a wet day. The remaining days were classified as dry days.

#### 2.4. Atmospheric Fields

The European Centre for Medium-Range Weather Forecasts ERA-Interim (Dee et al., 2011) reanalysis product was used to (1) determine the typical atmospheric conditions of dry seasons and rainy seasons, (2) determine differences in atmospheric conditions between rainy and dry days within rainy seasons, and (3) verify trends in rainfall. Daily zonal and meridional wind velocities and specific humidity were examined from 1983 to 2017 at 500 and 850 hPa. Vertical velocity at 500 hPa also was examined.

#### 2.5. Back Trajectory Analyses and Land Cover Information

In order to systematically evaluate air parcel origins throughout western Uganda, 7-day back trajectories specific to each rainfall region were created for every day from 1983 to 2017. The trajectories were produced using National Centers for Environmental Prediction Reanalysis 1 data (Kalnay et al., 1996) in the Hybrid Single-Particle Lagrangian Integrated Trajectory model, Version 4 (Stein et al., 2015) with the model vertical velocity option. Each trajectory began at 0900 UTC (12 noon local time) at 500 m above ground level at the centroid of a rainfall region. The trajectories terminating in each rainfall region were placed into clusters using the clustering procedure included in Hybrid Single-Particle Lagrangian Integrated Trajectory model.

The typical land cover characteristics, rainfall totals, and atmospheric conditions of the trajectories were calculated. The mean of CHIRPS and TAMSAT-2 values was used as the rainfall total. Land cover characteristics of trajectories were determined by calculating the proportion of the duration of a trajectory over various types of land cover. Since the time period was 1983–2017, the Moderate Resolution Imaging Spectroradiometer MCD12Q1.006 land cover type database for 2001 was used (Friedl et al., 2002, 2010). The database has a 500-m spatial resolution and consists of 17 type-1 land cover classes. Box plots of daily rainfall totals, 500-hPa specific humidity, 500-hPa vertical velocity, and 850-hPa specific humidity were produced using the daily ERA-Interim data. Finally, Student's *t* tests ( $\alpha = 0.05$ ; one tailed) were used to test for differences between the aforementioned rainfall and atmospheric variables between each of the trajectory types.

In order to examine seasonal differences among the trajectories, trajectory-cluster frequencies (i.e., frequencies of trajectory types) and associated rainfall totals (the mean of CHIRPS and TAMSAT-2) were calculated. Within each season, to assess whether a trajectory cluster had a disproportionately high or low frequency on rainfall days, chi-square tests ( $\alpha = 0.01$ ) were conducted. Contingency tables for the tests contained the following frequencies: (1) trajectories in the cluster on wet days; (2) trajectories in other clusters on wet days; (3) trajectories in the cluster on dry days; and (4) trajectories in other clusters on dry days.

#### 2.6. Trends in Rainy-Season Variables

Multidecadal trends in rainy-season variables were assessed. The variables were season onset, season cessation, season duration, seasonal rainfall total, and seasonal rainfall intensity. The intensity of rainfall represented the mean daily rainfall total within a season, and it was calculated by dividing the seasonal rainfall total by the number of days in the season. CHIRPS and TAMSAT-2 data—with the mean value for the day of year replacing invalid TAMSAT-2 values—were used to calculate two sets of variables, and the final values used in the trend analyses were the means of results from the two products. Trends over 1983–2017 of the rainy-season variables were assessed using Kendall-Tau correlation tests ( $\alpha = 0.05$ ; one tailed). The Kendall-Theil robust line, the median of the slopes between all combinations of two points in the data (Helsel & Hirsch, 2002), was used to estimate changes in the rainy-season variables over the 35-year period.

#### 2.7. Trends in and Correlations Between Seasonal Rainfall and Seasonal Atmospheric Conditions

Trends in rainfall for the standard climatological seasons (e.g., DJF), mean seasonal reanalysis atmospheric variables, and seasonal frequencies of trajectory types were analyzed for each rainfall region. The seasonal rainfall totals were the mean of CHIRPS and TAMSAT-2 rainfall totals. Data from ERA-Interim and an additional high-resolution product, Modern-Era Retrospective analysis for Research and Applications, Version 2 (MERRA-2) (Gelaro et al., 2017), were used to calculate the seasonal reanalysis variables. The seasonal reanalysis values were the mean of the two products. Trends over 1983–2017 were assessed using Kendall-Tau correlation tests ( $\alpha = 0.05$ ; one tailed). In addition, correlations over the 35 years between seasonal rainfall and reanalysis variables and trajectory-type frequencies were assessed using Pearson product-moment correlation tests ( $\alpha = 0.05$ ; one tailed).

### 3. Results

#### 3.1. General Characteristics of the Rainfall Regions

The regionalization procedure divided western Uganda into five homogeneous rainfall regions that represented latitudinal zones as well as the small portion of lowland rainforest in western Uganda (Figure 1). In general, elevation increases from north to south, with Region 1, the northernmost region, and Region 5, the southernmost region, having mean elevations of 898 and 1,584 m above sea level, respectively. Region 3 was relatively unique among the regions, not only because of its small size but also because of its location on the western side of the Rwenzori Mountains, which makes it similar to locales in the extreme eastern portion of the Congo Basin. Region 1 had an annual rainfall regime, with the one long rainy season occurring from late March to mid-November; approximately 90% of the annual rainfall occurred during the rainy season (Figure 2). The rest of the regions had biannual rainfall regimes, and, for those regions, the first rainy season typically occurred from MAM and the second rainy season typically began in early August and ended in either late November or early December (Figure 2). Nearly 80% of the annual rainfall occurred during the rainy seasons.

#### 3.2. Atmospheric Conditions of Rainy and Dry Seasons

Ascending air, increased specific humidity, and weak easterly/southeasterly lower troposphere flow occurred over western Uganda during the rainy seasons (Figure 3; even columns). During both rainy seasons that moist, rising air existed across CEA and was centered at the equator. The lower troposphere flow was generally southerly (westerly) over CEA and southeasterly over western Uganda during the first (second) rainy season (Figure 3b). The flow during the second rainy season was much weaker, with the winds over CEA shifting to westerlies. Much of EEA had weak sinking air and southeasterly flow during the western Uganda rainy seasons; the flow was much weaker than during the dry seasons.

Descending air, decreased specific humidity, and easterly/southeasterly lower troposphere flow occurred over western Uganda during the dry seasons (Figure 3; odd columns). During the first dry season, which primarily occurs during DJF, sinking, relatively dry air existed north of the equator and over EEA. Strong easterly flow occurred across northern EEA and Regions 1 and 2 of western Uganda, and weak flow was over CEA. During the second dry season, which occurs mostly during June and July, the dry, sinking air shifted to the Southern Hemisphere yet still remained over EEA. Strong southerly flow existed over EEA, and weak southerly/southeasterly flow existed over western Uganda and CEA.

#### 3.3. Atmospheric Conditions on Wet and Dry Days Within Rainy Seasons

For both rainy and dry seasons, wet days in western Uganda were characterized by increased ascending air and specific humidity compared to dry days (Figure 4). The largest anomalies were typically centered over western Uganda, since the composite maps were based on rainfall occurrence at the five rainfall regions there. Across all of western Uganda, wet days during the rainy (dry) seasons had 5% (11%) higher 850-hPa specific humidity compared to dry days. At the 500-hPa level (not shown), the wet days during rainy (dry) seasons had even larger percent increases in specific humidity (15% in rainy seasons and 24% in dry seasons). On wet days during the first dry season, increased lower troposphere specific humidity existed across northern tropical Africa and all of EEA. The zone of increased specific humidity was more confined to western Uganda during the first rainy season. And during the second dry and second rainy seasons, the increased specific humidity tended to occur in a zone that extended from southern CEA to northern EEA.

Westerly wind anomalies, based on wet days minus dry days, were prevalent across most of equatorial Africa during wet days in both rainy and dry seasons in western Uganda (Figure 4). At the 850-hPa level, wet days during the first dry season had southwesterly/westerly anomalies over CEA and southerly anomalies over EEA. First-rains wet days had 850-hPa westerly anomalies over CEA and western Uganda, while southerly anomalies tended to occur over EEA. Wet days during both the second dry and second rainy seasons had 850-hPa westerly anomalies over CEA and western Uganda, with northerly anomalies over EEA.

#### 3.4. Back Trajectories for the Rainfall Regions

There were eight major types of air-parcel trajectories affecting western Uganda, and they differed substantially in terms of the types of land cover that the air parcels crossed (Figures 5 and 6). The trajectory types, named after the general geographical origin of the air parcels, were as follows: northerly (N),

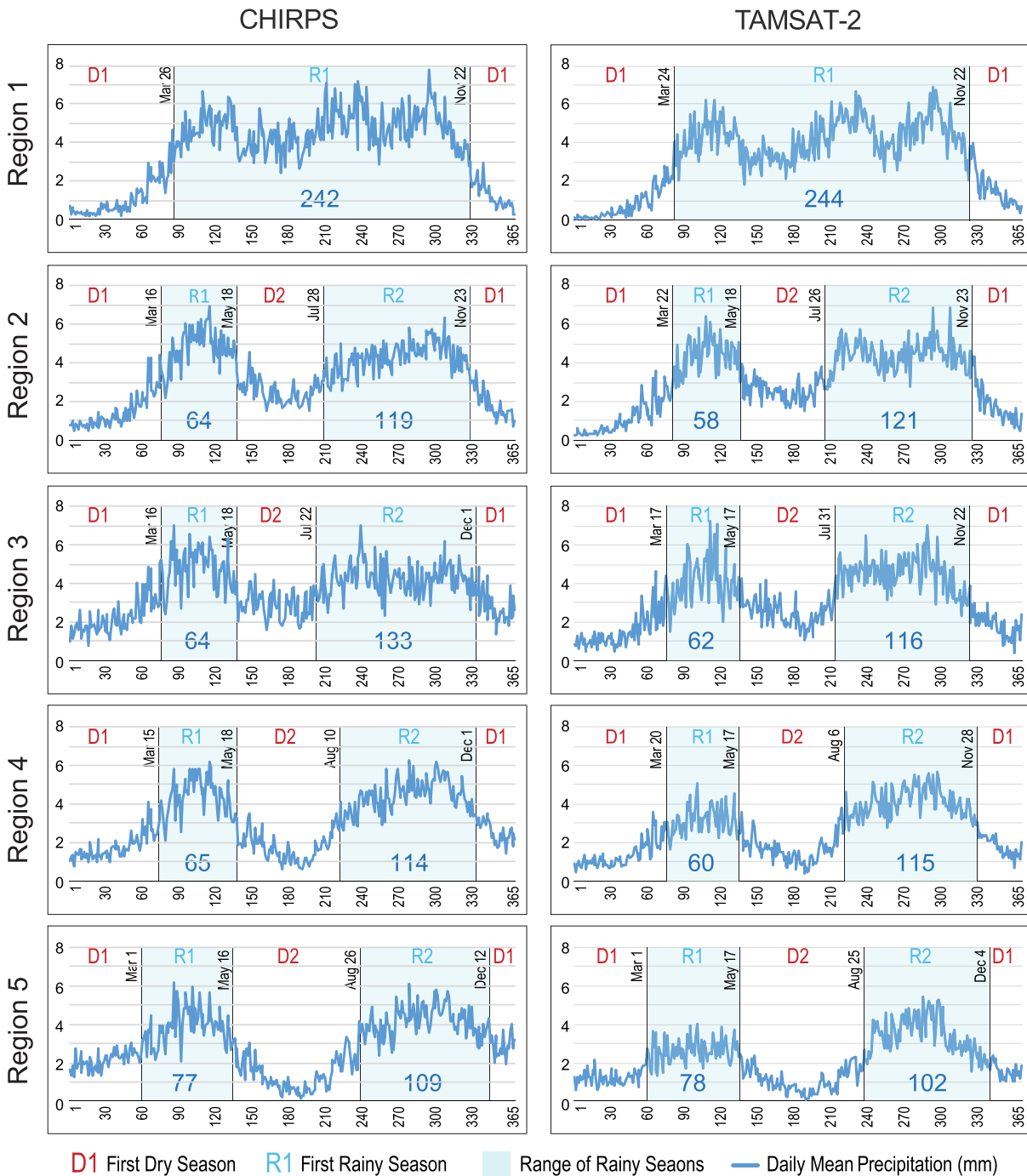


**Figure 2.** Typical mean daily rainfall, rainy-season onset and cessation dates, rainy-season duration for the five rainfall regions for 1983–2017 for the two rainfall products. Dates are in black and durations (in days) are in blue.

northeasterly (NE), easterly (E), southeasterly (SE), southerly (S), southwesterly (SW), westerly (W), and local (L). N trajectories arrived mostly from the Sahara desert and were rare for all regions. NE trajectories, which extended over the North Indian Ocean toward the Arabian Sea, decreased greatly in frequency when moving from the northern to southern regions. NE trajectories were typically over oceans for half the hours. E trajectories—which were relatively infrequent—also tended to originate over the Indian Ocean; however, most of the hours of the E trajectories were over land, primarily shrublands,

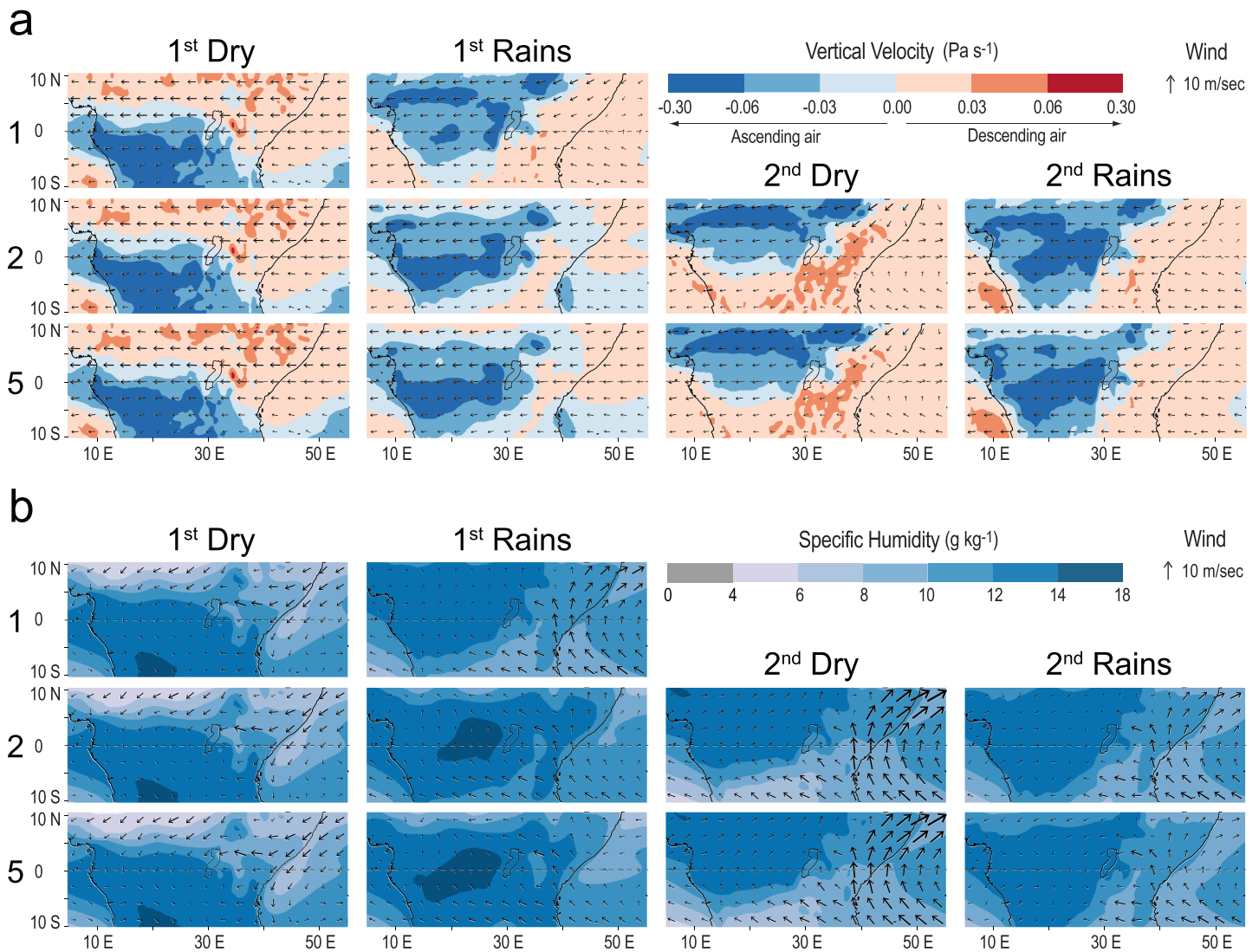


**Figure 3.** Mean seasonal (a) 500-hPa vertical velocity and wind vectors and (b) 850-hPa specific humidity and wind vectors for Regions 1, 2, and 5. The outline of western Uganda is shown in black. The rainy-season periods are typically as follows: late March to late November for Region 1; mid-March to mid-May (first rains) and late July to late November (second rains) for Region 2; and early March to mid-May (first rains) and late August to early December (second rains).

savannas, and grasslands. SE trajectories was the most common trajectory type, occurring on 29% of all days on average across the regions. These trajectories originated in the South Indian Ocean and generally had approximately the same number of hours over ocean and land. S trajectories were similar to SE trajectories, but they occurred much less frequently and had a higher percentage of hours over the ocean. Both SW and W trajectories were relatively slow and, unlike the other trajectories, were typically present over the evergreen broadleaf forests of the Congo basin for at least 70% of the hours. W trajectories dwelled over evergreen broadleaf forests for approximately 80% of the hours. Therefore, W trajectories also can be referred to as Congo westerlies. These trajectories occurred on 23% of the days on average across the regions and were thus the second most frequent trajectory type. There was an increased frequency of both SW and W trajectories when moving from north to south: W trajectories were the most prevalent trajectories in Regions 3 and 5, where they occurred on nearly 30% of days. Finally, L trajectories originated in or near western Uganda and did not have a directional component.

The atmospheric conditions of the trajectory clusters differed in the following ways: N and NE trajectories were much drier and stable than the other trajectories and Congo westerlies were the wettest and most unstable of the trajectories (Figure 7). N and NE trajectories were unique among the trajectories, with

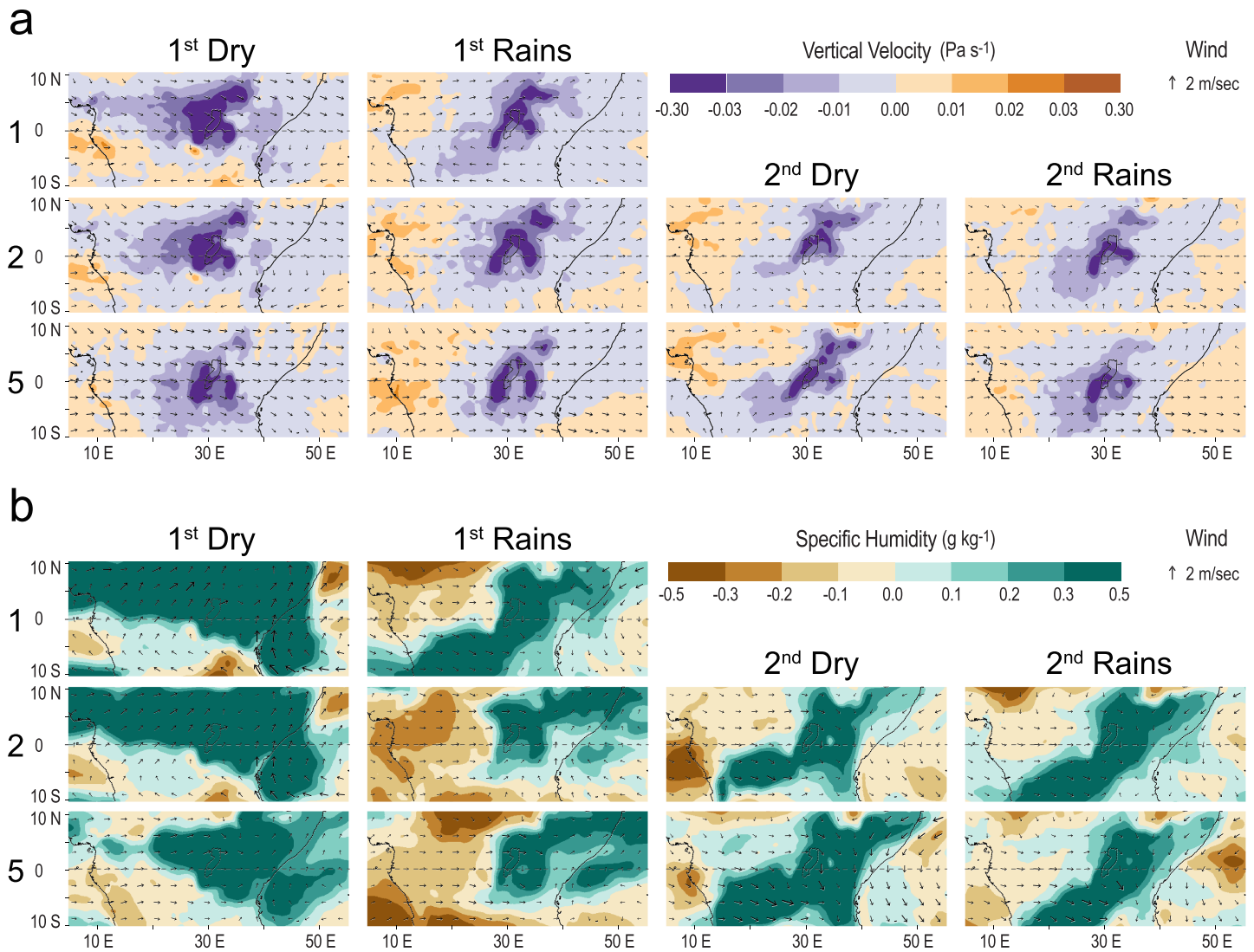


**Figure 4.** Differences for each season between wet days and dry days in (a) 500-hPa vertical velocity and wind vectors and (b) 850-hPa specific humidity and wind vectors for Regions 1, 2, and 5. The outline of western Uganda is shown in black. The rainy-season periods are typically as follows: late March to late November for Region 1; mid-March to mid-May (first rains) and late July to late November (second rains) for Region 2; and early March to mid-May (first rains) and late August to early December (second rains).

those trajectories being the only ones associated with middle-troposphere vertical descent as well as having lower mean daily rainfall totals and specific humidity than the other trajectory clusters. Congo westerlies had significantly higher mean daily rainfall, significantly more negative vertical motion, and significantly more 500-hPa specific humidity than the other trajectory clusters. Congo westerlies did not have the highest 850-hPa specific humidity.

There was a strong seasonality to the trajectories, and there were major differences among trajectory types with respect to rainfall contribution within seasons (Figure 8). NE trajectories were most common in Regions 1 and 2; since they occur mostly during the first dry season, these trajectories contribute very little to rainfall totals. SE trajectories, which were common throughout western Uganda in all seasons but the first dry season, were major contributors to rainfall during rainy seasons. Over 10% of the annual rainfall in all regions occurred on SE trajectory days during the first rainy season, and over 40% of the first-rains rainfall occurred on those days. SE trajectories contributed less to rainfall in the second rains when moving to Regions 3–5. W trajectories occurred in all seasons but were extremely prevalent during the second rainy season, where they contributed substantially to rainfall. In Regions 3–5, W trajectories were the dominant

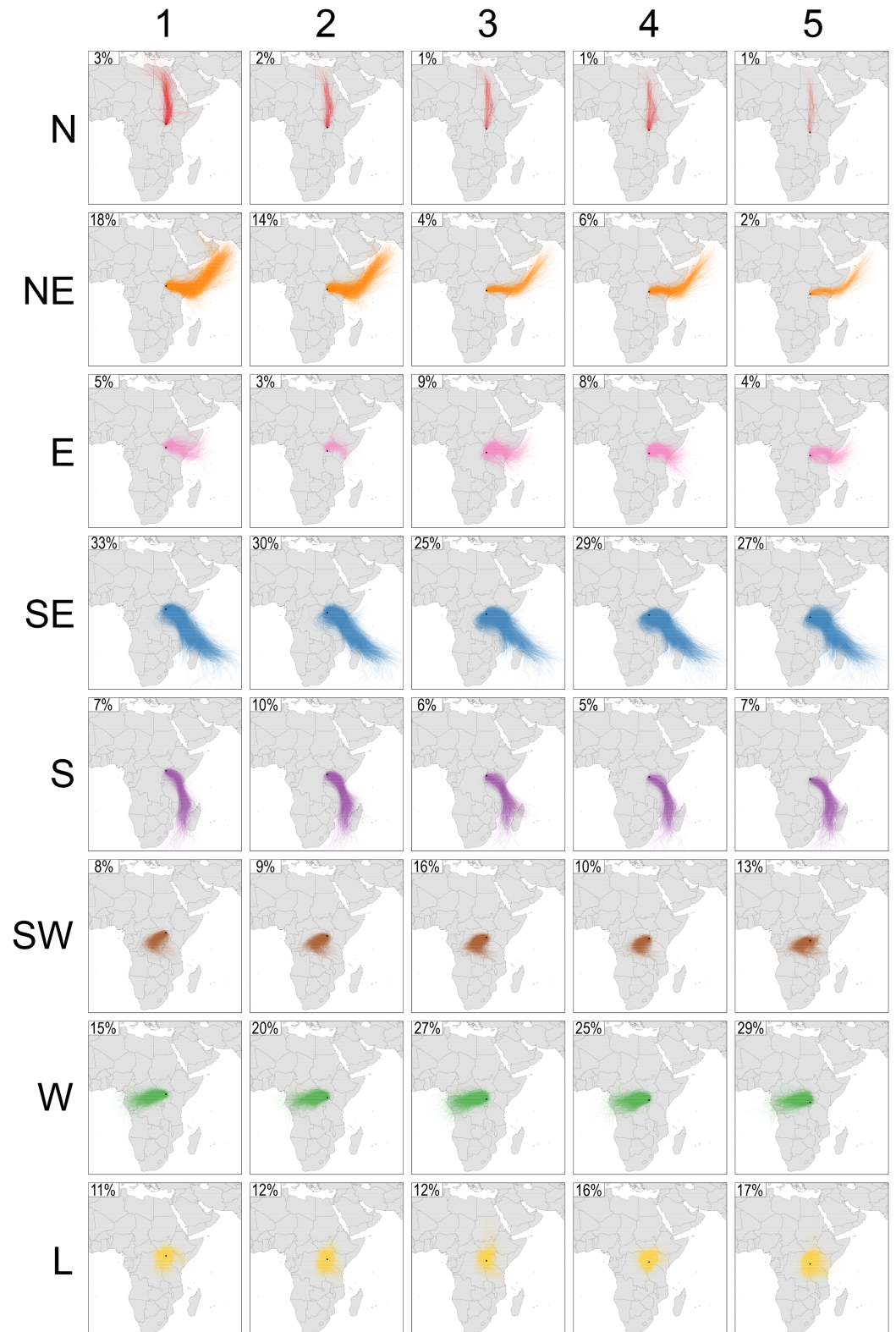


**Figure 5.** The eight clusters of 7-day back trajectories. All trajectories from 1983 to 2018 are shown for the five rainfall regions. The trajectory clusters are northerly (N), northeasterly (NE), easterly (E), southeasterly (SE), southerly (S), southwesterly (SW), westerly (W), and local (L). Percentages of days for a region on which the trajectory cluster occurred are shown.

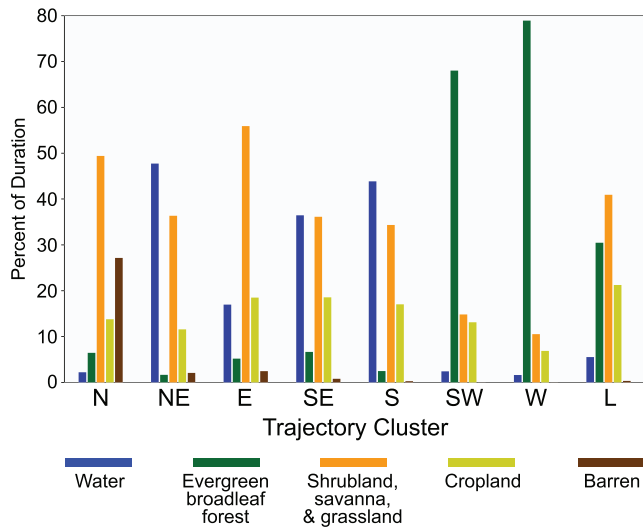


**Figure 6.** Percent of trajectory duration spent over various types of land cover. Percentages are the mean values from all trajectories for the five regions.

contributor to second-rains rainfall. Over 20% of the annual rainfall in these regions occurred on W trajectory days during the second rainy season, and over 40% of the second-rains rainfall occurred on those days.

There was a dramatic difference between westerly/southwesterly trajectories and other trajectories with respect to occurrences on wet and dry days within the seasons (Figure 9). We define a wet (dry) trajectory as one that has a disproportionately high frequency on wet (dry) days, based on the results of the chi-square tests. SW and W trajectories were wet trajectories during most seasons, and this is especially true for W trajectories during the second dry and second rainy seasons. N and NE trajectories were typically dry trajectories, especially during the first dry season. SE and S trajectories were wet trajectories at the northernmost regions during the first dry season but shifted to dry trajectories for all regions during the second dry and second rainy seasons (which is equivalent to the first rains at Region 1).

### 3.5. Trends in Rainy-Season Variables

While Region 1, the only region with a single rainy season, only had a slight lengthening of the rainy season from 1983 to 2017, there were large increases in total rainfall and rainfall intensity over that period (Table 1).

The rainy season increased by roughly 11 days, and the increase was not significant. Trends in both rainfall total and rainfall intensity were significant. Seasonal rainfall increased by 20%, which translates into an increase of 58 mm per decade.

The first rains among the biannual rainfall regions (Regions 2 to 5) had large increases in duration and rainfall totals (Table 1). The first rains increased in duration from 22 to 34 days, and these increases were significant for all four regions. The mean increase was approximately 1 week per decade. All regions had either a significant decrease in onset or a significant increase in cessation or both; the northern regions had a significant increase in cessation, and the southern regions had a significant decrease in cessation. The mean decrease in onset was 16 days, and the mean increase in cessation was 12 days. All four regions had significant increases in rainfall totals, with totals increasing by 52% to 83%. The mean increase in rainfall total was 45 mm per decade. There were no significant changes in rainfall intensity.

Compared to the first rains, the second rains had much weaker changes in season onset, cessation, duration, and rainfall total, but the increase in rainfall intensity was much greater (Table 1). With the exception of Region 5, the biannual rainfall regions tended to have decreased season onset offset greatly by a decreased season cessation; as a result, season duration did not change. Region 5 had a significant increase in season duration of 20 days (i.e., 6 days per decade), with decreasing season onset more responsible than increasing season cessation. Resulting from the increased duration, Region 5 also was the only region to have a significant increase in rainfall total: The total increased by 31% over the 35 years (i.e., 34 mm per decade). Finally, all regions except Region 5 had significant increases in rainfall intensity.

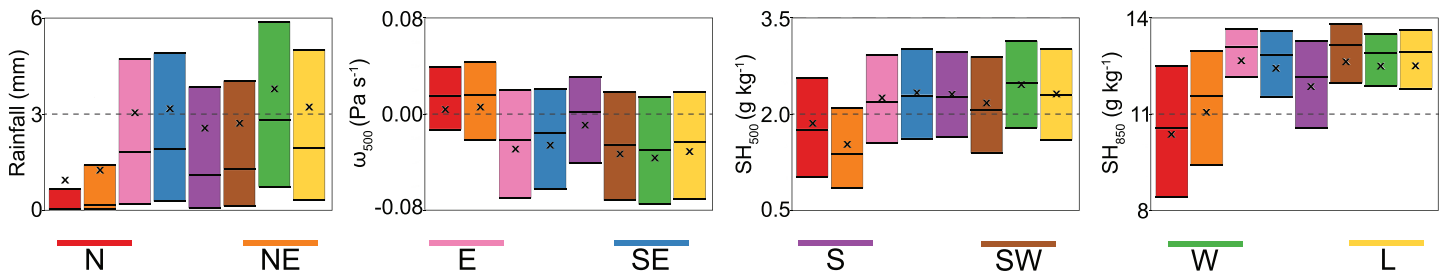


**Figure 7.** Box plots of daily rainfall, 500-hPa vertical velocity ( $\omega_{500}$ ), 500-hPa specific humidity ( $SH_{500}$ ), and 850-hPa specific humidity ( $SH_{850}$ ). The black horizontal lines are the first quartile, median, and third quartile. The mean is denoted by an x.

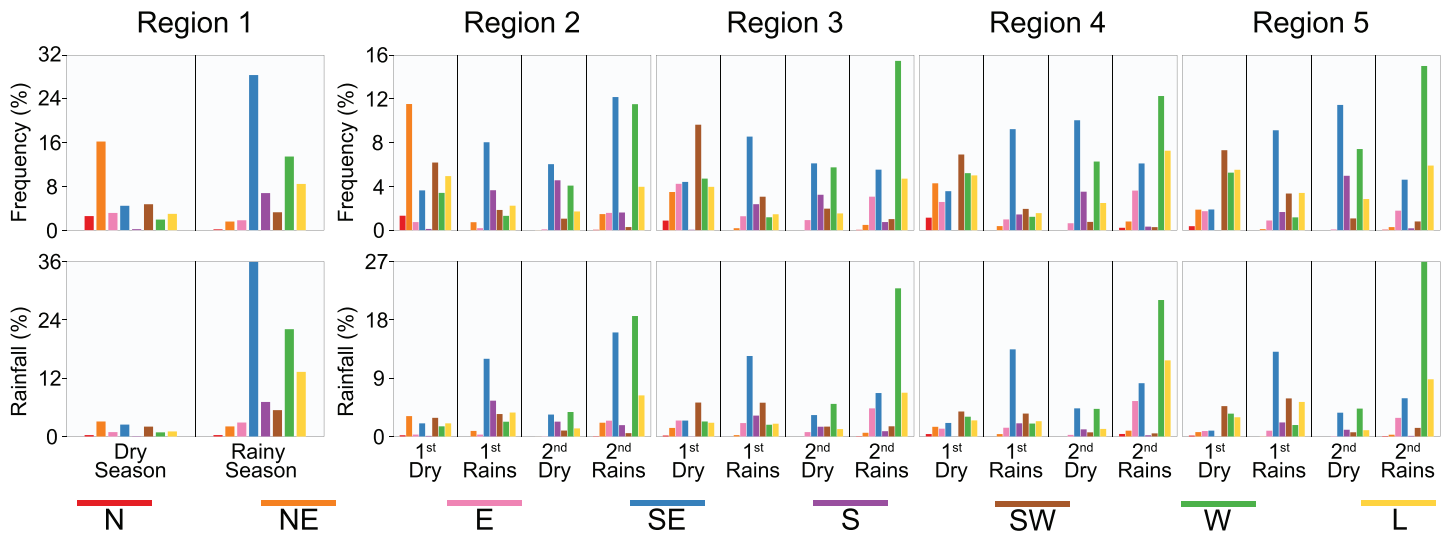


**Figure 8.** Trajectory occurrence and associated rainfall during the seasons for the five regions. The values are percentages of total annual occurrence and rainfall. The rainy-season periods are typically as follows: late March to late November for Region 1; mid-March to mid-May (first rains) and late July or early August to late November (second rains) for Regions 2–4; and early March to mid-May (first rains) and late August to early December (second rains) for Region 5.

### 3.6. Trends and Correlations for Climatological Seasons

Nearly all seasons, except DJF, experienced wetting trends in all regions, and the cumulative effect is that western Uganda had at least a 14% increase in rainfall from 1983 to 2017 (Figure 10a). Most regions had significant rainfall increases during MAM, JJA, and SON. Region 5, the southernmost region, was unique among the regions, with an additional significant rainfall increase during DJF. Annual rainfall in that region increased by 24%.

Changes in middle-troposphere conditions supported the changes in rainfall (Figure 10b). While results using the mean of ERA-Interim and Modern-Era Retrospective analysis for Research and Applications, Version 2 are shown in Figure 10, those two products did have similar correlations and trends for the 500- and 850-hPa variables (Figure S1 in the supporting information). The 500-hPa specific humidity was significantly positively correlated with seasonal rainfall in all seasons for all regions, and it had significantly increasing trends in all regions during MAM, JJA, and SON. 500-hPa vertical velocity was significantly negatively correlated with rainfall in nearly all seasons across the five regions, and significant decreasing trends (more upward motion) occurred in JJA and SON for all regions. All regions except Region 5 had additional significantly decreasing trends in MAM, while the northern regions had significant increasing trends (less upward motion) in DJF.

Changes in lower troposphere specific humidity supported the increases in rainfall during JJA and the lack of rainfall increase during DJF (Figure 10b). 850-hPa specific humidity was significantly positively correlated with rainfall in JJA in all regions, and all regions except Region 1 had significant increasing trends in specific humidity during JJA. Nearly all regions had significant positive correlations between 850-hPa specific humidity and rainfall in DJF, and all trends in specific humidity were significantly negative. There were negative trends in 850-hPa specific humidity during MAM in all regions.

There were mostly shifts toward more westerly lower troposphere flow, and that change supported the rainfall changes (Figure 10b). Rainfall and 850-hPa zonal velocity in JJA were significantly correlated in all regions, and there was a significant positive trend in zonal velocity (i.e., increasing westerly or decreasing easterly flow). All regions except Region 3 had significantly positive correlations in SON, and Regions 4 and 5 had an additional significant positive correlation in MAM. The 850-hPa zonal velocity had a significantly positive trend for all of the above region/season combinations except SON in Region 2. Region 3 had a significant negative correlation between DJF rainfall and 850-hPa zonal velocity, and the negative trend in zonal flow also was significant.

Changes in Congo westerlies did not align well with changes in lower troposphere zonal flow and thus did not support the rainfall changes (Figure 10b). Shown below Congo westerlies in Figure 10b are correlations

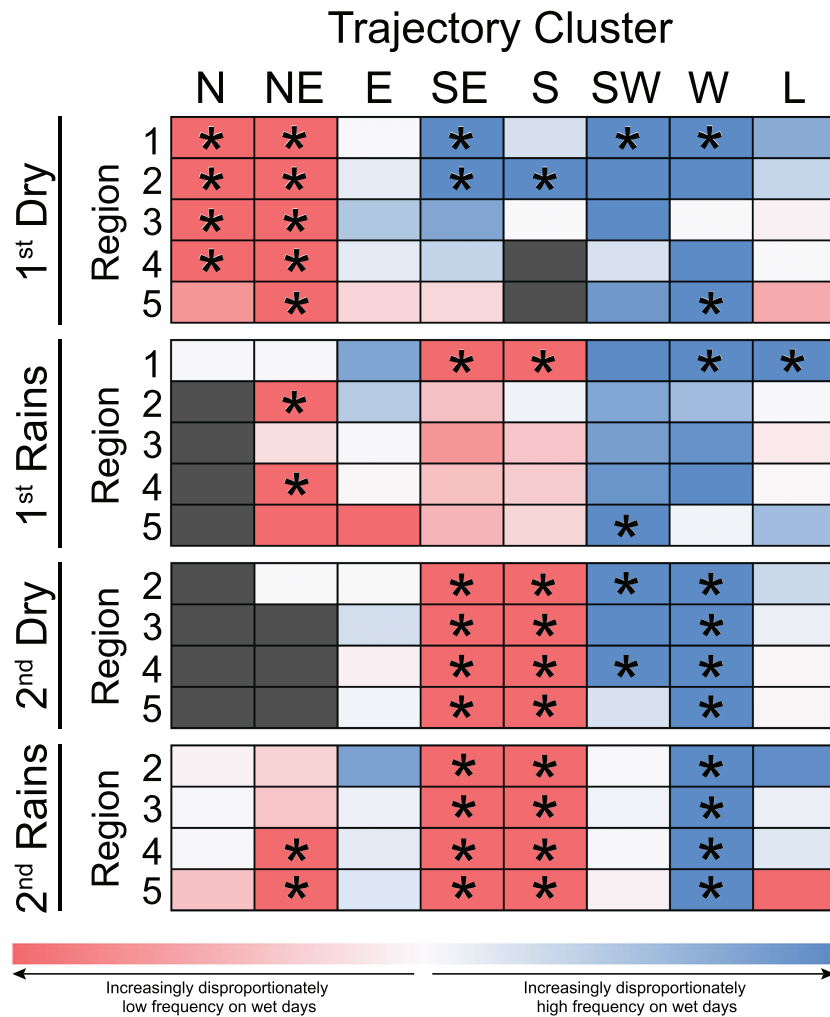


**Figure 9.** Chi-square statistics (the mean of the statistics from the separate analyses involving CHIRPS and TAMSAT-2 data) for all trajectory/season combinations in the five regions. The white to red (blue) range indicates an increasingly disproportionately low (high) frequency of a trajectory cluster on wet days. Gray indicates no trajectories for that cluster/season/region combination. Asterisks indicate that both CHIRPS and TAMSAT-2 chi-square statistics are significant at the 0.01 level. The rainy-season periods are typically as follows: late March to late November for Region 1; mid-March to mid-May (first rains) and late July or early August to late November (second rains) for Regions 2–4; and early March to mid-May (first rains) and late August to early December (second rains) for Region 5.

and trends for EB<sub>80</sub> trajectories, which are trajectories with at least 80% of hours over evergreen broadleaf forest (i.e., Congo rainforest). EB<sub>80</sub> trajectories, which occurred on 21% of the days on average across the regions, were 73% Congo westerlies, 21% SW trajectories, and 6% L trajectories. Rainfall and the frequency of Congo westerlies and EB<sub>80</sub> trajectories in JJA in the northern regions were significantly positively correlated, but the trends in westerlies were not significant. Significant negative correlations occurred in MAM and SON in Region 3 for Congo westerlies and in SON for EB<sub>80</sub> trajectories; however, those variables did not have significant trends. The only significant trends in Congo westerlies were negative trends during SON in Regions 4 and 5. And the only significant trends in EB<sub>80</sub> trajectories were positive trends in DJF in Regions 3–5.

#### 4. Discussion

This study found that intra-annual variability of rainfall and the atmospheric conditions of seasons in western Uganda is much more similar to CEA than to EEA. Previously, western Uganda has been considered both a part of CEA and EEA, but both regions are impacted by the equinoctial crossing of the tropical

**Table 1**

*Changes in Rainy-Season Onset, Cessation, Duration, Rainfall Total, and Rainfall Intensity (i.e., Mean Daily Rainfall) From 1983 to 2017*

	Onset (days)	Cessation (days)	Duration (days)	Rainfall total (mm)	Rainfall intensity (mm)
First rains					
Region 1	−4	8	11 (5)	204 <sup>a</sup> (20)	0.56 <sup>a</sup> (13)
Region 2	−9	16 <sup>a</sup>	22 <sup>a</sup> (45)	134 <sup>a</sup> (52)	−0.15 (−3)
Region 3	−18 <sup>a</sup>	15 <sup>a</sup>	34 <sup>a</sup> (68)	189 <sup>a</sup> (85)	0.20 (4)
Region 4	−17 <sup>a</sup>	8	26 <sup>a</sup> (59)	123 <sup>a</sup> (62)	−0.09 (−2)
Region 5	−18 <sup>a</sup>	11	27 <sup>a</sup> (50)	142 <sup>a</sup> (83)	0.49 (14)
Second rains					
Region 2	−13	−3	5 (5)	104 <sup>a</sup> (21)	0.44 <sup>a</sup> (10)
Region 3	−6	−5	3 (2)	45 (9)	0.39 <sup>a</sup> (9)
Region 4	11	−10	−3 (−3)	43 (9)	0.57 <sup>a</sup> (14)
Region 5	−11	7	20 <sup>a</sup> (19)	118 <sup>a</sup> (31)	0.38 (10)

Note. The percentage change from 1983 to 2017 is shown parentheses for duration, rainfall total, and rainfall intensity.

<sup>a</sup>Significant trends ( $\alpha = 0.05$ ; one tailed).

rainbelt and have more rainfall in SON than in MAM (Washington et al., 2013). EEA has more rainfall in MAM than in SON (Camberlin et al., 2009). For rainy seasons in western Uganda, the differences in 500-hPa vertical velocity, 850-hPa specific humidity, and 850-hPa winds between western Uganda and CEA are small, while the differences in values between western Uganda and EEA are much larger (e.g., EEA had descending air during the rainy seasons; Figure 3).

Congo westerlies dominate during the second rainy season and are important features during wet days in all seasons. This supports previous findings of Congo westerlies occurring throughout the year and being most developed in July–September (Nicholson & Grist, 2003). And the Congo Basin as a moisture source is much more likely in SON than MAM (Hua et al., 2019). Differences in circulation between wet days and dry days produced 850-hPa westerly anomalies for all seasons, with the possible exception of boreal winter in northwestern Uganda (Figure 4). Wet days and spells within rainy seasons in western EEA (e.g., western Kenya) also have been shown to have westerly anomalies (Camberlin, 1997; Camberlin & Wairoto, 1997; Pohl & Camberlin, 2006a, 2006b). The W trajectories presented in this paper represent Congo westerlies; these trajectories spend on average at least 80% of the time over the Congo rainforest. Therefore, they likely are transporting recycled moisture (i.e., evapotranspired moisture from the Congo rainforest) into western Uganda (Dyer et al., 2017). As result, Congo westerlies are more unstable and have higher middle-troposphere moisture levels than the other trajectories (Figure 7). Congo westerlies have a disproportionately high frequency on wet days in most region/season combinations, especially the second dry and second rainy seasons in the biannual-regime regions. Congo westerlies are associated with at least 40% of the rainfall during the second rainy season in the southern regions; in the southernmost region, the value could exceed 60%. Since it has been postulated that air that has passed over extensive tropical vegetation in the preceding few days should produce greatly increased rainfall totals (Spracklen et al., 2012), the potentially large impact of Congo westerlies on western Uganda rainfall is not unexpected.

The rainy seasons, especially the first rains, have gotten longer and have had increased rainfall over the past several decades. With the exception of Region 1, which has an annual rainfall regime, the first rains increased in duration on average by four weeks over the 35 years; as a result, the rainfall totals in the first rains increased by over 50%. The large increases in the first rains also were found by Salerno et al. (2019) for locales within our Regions 2–4. The earlier onset and later cessation of the first rains is supported by the significant increases in rainfall in MAM (Figure 10a). The second rains had smaller increases in rainfall (i.e., a mean increase of 18%). Since JJA had significant rainfall increases and the typical onset of the second rains was in August, it makes sense that the onset for the second rains decreased by approximately 10 days over the 35 years. With the typical cessation date of the second rains occurring in late November and no significant increase in DJF rainfall, the cessation date of the second rains essentially did not change. But the increased SON rainfall did contribute to the significant increases in mean daily rainfall totals during the second rains.

Increased rainfall in MAM, JJA, and SON—and thus by extension the short rains and long rains—is supported primarily by changes in middle-troposphere conditions and also by changes in lower troposphere

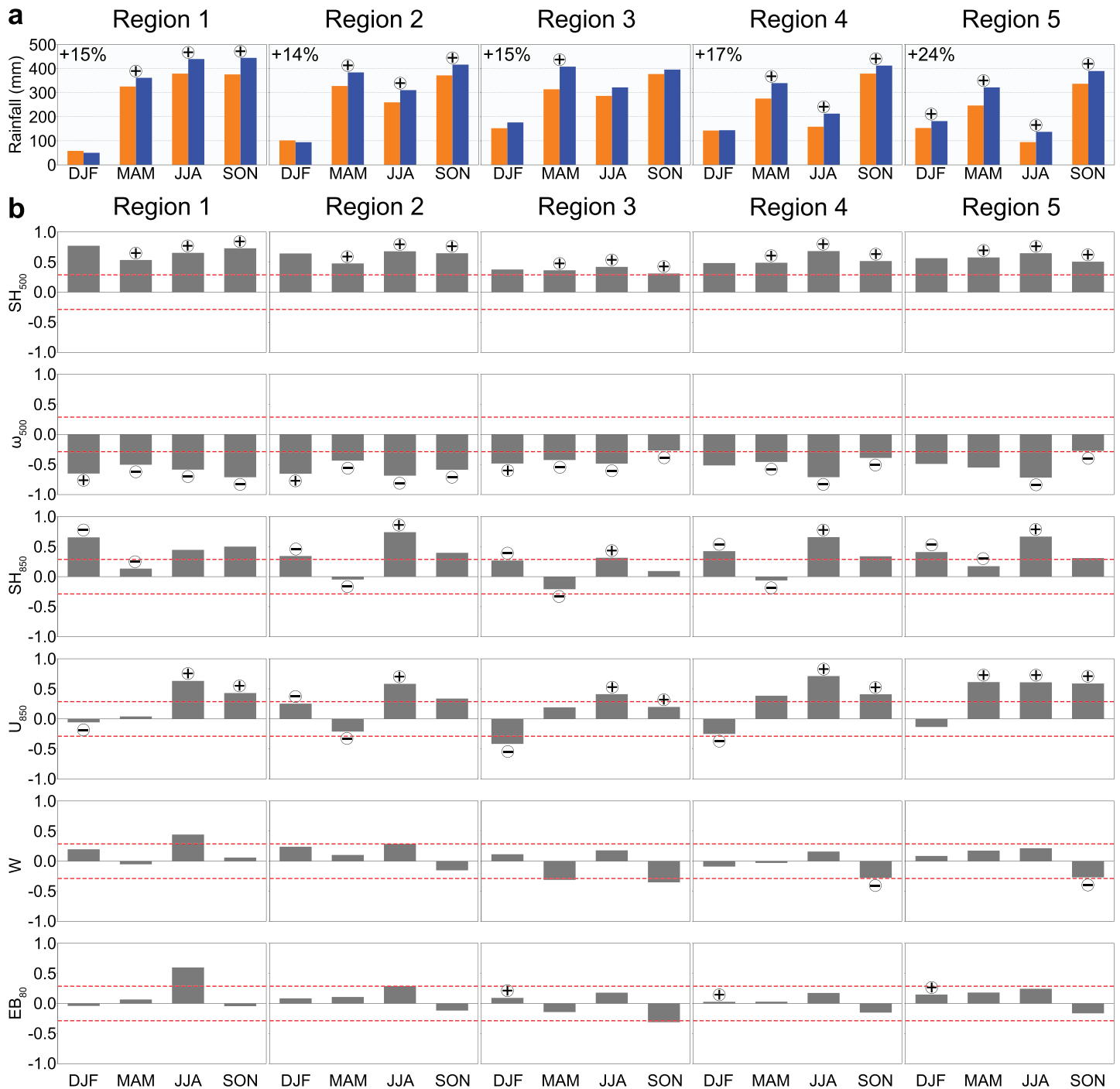


**Figure 10.** (a) Projected seasonal rainfall totals for 1983 (orange bars) and 2017 (blue bars). Projected values are derived from the Kendall-Theil robust line. Plus signs indicate seasons that had a significant ( $\alpha = 0.05$ ; one-tailed) increase in rainfall. Values in the upper-left corner of each panel are the percent increase in annual rainfall from 1983 to 2017. (b) Pearson product-moment correlation coefficients between seasonal rainfall and 500-hPa specific humidity ( $SH_{500}$ ), 500-hPa vertical velocity ( $\omega_{500}$ ), 850-hPa specific humidity ( $SH_{850}$ ), 850-hPa zonal velocity ( $U_{850}$ ), frequency of westerly trajectories (W), and EB<sub>80</sub> trajectories (i.e., trajectories with at least 80% of hours over evergreen broadleaf forest). Coefficients beyond the dashed red lines are significant ( $\alpha = 0.05$ ; one-tailed). Plus (minus) signs indicate seasons that had a significant ( $\alpha = 0.05$ ; one-tailed) increases (decreases).

flow. Over western Uganda, there was a significant increase in 500-hPa specific humidity in all seasons except DJF and a significant increase in 500-hPa upward motion in JJA and SON and to a lesser degree in MAM. In addition, there was a shift toward more westerly lower troposphere flow in JJA in the northern

regions and in both JJA and SON in the southern regions. And across the five regions of western Uganda, a majority of the seasons with significant trends also had significant correlations with rainfall totals.

Aligning with the current trends discussed above, global climate models project an increased rainfall for western Uganda in the future. Based on results from an ensemble of global climate models, rainfall in western Uganda is projected to increase 0.9 mm/day by the late 21st century compared to the late 20th century, and the possible cause of the increase in the eastern Congo Basin is increased middle-troposphere moisture convergence (Creese et al., 2019). The above increase in rainfall translates to an increase of 8.8 mm per decade, which appears reasonable, since the mean trend in this paper for SON over 1983–2017 was 12.5 mm per decade.

Given the strong impact that Congo westerlies have on wet days in both rainy and dry seasons, it is perplexing that a strong relationship does not exist between Congo-westerly frequencies and the increased rainfall. Congo westerlies have not increased in frequency in any season. In fact, westerlies have decreased in SON in Regions 4 and 5; this coincides with the second rains, when Congo westerlies are the largest contributors to rainfall among the trajectories. Nevertheless, there are strong correlations in Region 1 between JJA rainfall and the frequencies of Congo westerlies and trajectories that spent at least 80% of hours over the Congo rainforest. In fact, over 40% of the rainfall in that season occurs on Congo-westerly days. It is possible that the Congo westerlies were not defined at an adequate precision or identified with the same accuracy over the 35 years or both. Then again, except for JJA in northwestern Uganda, there may simply not be a strong positive interannual relationship between Congo westerlies—no matter how they are identified—and rainfall.

## 5. Conclusions

Determining changes in timing, duration, and rainfall totals of rainy seasons is important in western Uganda, given the critical impact of rainfall on the millions of people in the region subsisting on rainfed small-scale farming. Rainfall has increased significantly in most climatological seasons throughout western Uganda; as a result, the two rainy seasons have gotten longer and wetter. Excluding extreme northwestern Uganda, which has an annual rainfall regime, the first rains—which on average over 1983–2017 have begun in the middle of March and ended in the middle of May—have increased in duration by 27 days and have had a 71% increase in rainfall from 1983 to 2017, while the second rains—which on average have begun in early August, except for a later start in southwestern Uganda, and ended in late November—have had varied changes in duration across western Uganda and have had a modest 18% increase in rainfall. But the second rains have had significant increases mean daily rainfall (i.e., rainfall intensity). Congo westerlies are associated with wet days in all seasons, and they are the largest contributor to rainfall during the second rains. However, the frequency of Congo westerlies does not appear to be related to interannual rainfall variability—and thus not the cause of increased rainfall—in western Uganda. This region, with a wetting trend rather than a drying trend, appears to be unique in equatorial Africa. And one cannot assume that the increased rainfall and longer rainy seasons benefits small-holder farmers. Increased rainfall may increase chances of fungal disease in crops and decrease the lack of time for proper harvesting of crops (e.g., maize).

This study acts as foundation for our current and future rainfall-agriculture research throughout western Uganda. As this study has shown, much more detailed information about moisture sources of rainfall in western Uganda is needed. Therefore, we are collecting rainwater from multiple sites for stable-isotopes analyses, and those analyses will be combined with back trajectory analyses. In addition, farmers throughout western Uganda have been interviewed and completed surveys to determine their perceptions of rainfall trends and how they are coping with those perceived changes (e.g., earlier onset and more seasonal rainfall) in rainfall.

## References

- Badr, H. S., Zaitchik, B. F., & Dezfuli, A. K. (2015). A tool for hierarchical climate regionalization. *Earth Science Informatics*, 8(4), 949–958. <https://doi.org/10.1007/s12145-015-0221-7>
- Camberlin, P. (1997). Rainfall anomalies in the source region of the Nile and their connection with the Indian summer monsoon. *Journal of Climate*, 10(6), 1380–1392. [https://doi.org/10.1175/1520-0442\(1997\)010<1380:RAITSR>2.0.CO;2](https://doi.org/10.1175/1520-0442(1997)010<1380:RAITSR>2.0.CO;2)
- Camberlin, P., Moron, V., Okoola, R., Philippon, N., & Gitau, W. (2009). Components of rainy seasons' variability in equatorial East Africa: onset, cessation, rainfall frequency and intensity. *Theoretical and Applied Climatology*, 98(3-4), 237–249. <https://doi.org/10.1007/s00704-009-0113-1>
- Camberlin, P., & Philippon, N. (2002). The East African March–May rainy season: Associated atmospheric dynamics and predictability over the 1968–97 period. *Journal of Climate*, 15(9), 1002–1019. [https://doi.org/10.1175/1520-0442\(2002\)015<1002:TEAMMR>2.0.CO;2](https://doi.org/10.1175/1520-0442(2002)015<1002:TEAMMR>2.0.CO;2)

### Acknowledgments

This research was supported by the National Science Foundation (Award 1740201) and approved by the Uganda National Council for Science and Technology. CHIRPS and TAMSAT-2 data were obtained from the International Research Institute for Climate and Society and are available at the website (<https://iridl.ldeo.columbia.edu/>). ERA-Interim data were obtained from the European Centre for Medium-Range Weather Forecasts and are available at the <https://www.ecmwf.int/en/forecasts/datasets/reanalysis-datasets/era-interim> website. MERRA-2 data were obtained from the NASA Goddard Earth Sciences Data and Information Services Center and are available at the website (<https://disc.gsfc.nasa.gov/daac-bin/FTPSubset2.pl>). Daily and monthly rainfall/atmospheric data for the rainfall regions in this manuscript—as well as geo-spatial data for the regions—can be accessed at the <https://data.mendeley.com/datasets/cbntk7yn/1> website.

- Camberlin, P., & Wairoto, J. G. (1997). Intraseasonal wind anomalies related to wet and dry spells during the “long” and “short” rainy seasons in Kenya. *Theoretical and Applied Climatology*, *58*(1-2), 57–69. <https://doi.org/10.1007/BF00867432>
- Christy, J. R. (2013). Monthly temperature observations for Uganda. *Journal of Applied Meteorology and Climatology*, *52*(10), 2363–2372. <https://doi.org/10.1175/JAMC-D-13-012.1>
- Cooper, P. J. M., Dimes, J., Rao, K. P. C., Shapiro, B., Shiferaw, B., & Twomlow, S. (2008). Coping better with current climatic variability in the rain-fed farming systems of sub-Saharan Africa: An essential first step in adapting to future climate change? *Agriculture, Ecosystems & Environment*, *126*(1-2), 24–35. <https://doi.org/10.1016/j.agee.2008.01.007>
- Costa, K., Russell, J., Konecky, B., & Lamb, H. (2014). Isotopic reconstruction of the African Humid Period and Congo air boundary migration at Lake Tana, Ethiopia. *Quaternary Science Reviews*, *83*, 58–67. <https://doi.org/10.1016/j.quascirev.2013.10.031>
- Creese, A., & Washington, R. (2018). A process-based assessment of CMIP5 rainfall in the Congo Basin: The September–November rainy season. *Journal of Climate*, *31*(18), 7417–7439. <https://doi.org/10.1175/JCLI-D-17-0818.1>
- Creese, A., Washington, R., & Munday, C. (2019). The plausibility of September–November Congo Basin rainfall change in coupled climate models. *Journal of Geophysical Research: Atmospheres*, *124*, 5822–5846. <https://doi.org/10.1029/2018JD029847>
- Dee, D. P., Uppala, S. M., Simmons, A. J., Berrisford, P., Poli, P., Kobayashi, S., et al. (2011). The ERA-Interim reanalysis: Configuration and performance of the data assimilation system. *Quarterly Journal of the Royal Meteorological Society*, *137*(656), 553–597. <https://doi.org/10.1002/qj.828>
- Dezfuli, A. (2017). Climate of Western and central equatorial Africa. In *Oxford Research Encyclopedia of Climate Science* (Vol. 1). Oxford, UK: Oxford University Press. <https://doi.org/10.1093/acrefore/9780190228620.013.511>
- Dezfuli, A. K., & Nicholson, S. E. (2013). The relationship of rainfall variability in western equatorial Africa to the tropical oceans and atmospheric circulation. Part II: The boreal autumn. *Journal of Climate*, *26*(1), 66–84. <https://doi.org/10.1175/JCLI-D-11-00686.1>
- Diem, J. E., Hartter, J., Salerno, J., McIntyre, E., & Grandy, A. S. (2017). Comparison of measured multi-decadal rainfall variability with farmers’ perceptions of and responses to seasonal changes in western Uganda. *Regional Environmental Change*, *17*(4), 1127–1140. <https://doi.org/10.1007/s10113-016-0943-1>
- Diem, J. E., Konecky, B. L., Salerno, J., & Hartter, J. (2019). Is equatorial Africa getting wetter or drier? Insights from an evaluation of long-term, satellite-based rainfall estimates for western Uganda. *International Journal of Climatology*, *39*(7), 3334–3347. <https://doi.org/10.1002/joc.6023>
- Diem, J. E., Ryan, S. J., Hartter, J., & Palace, M. W. (2014). Satellite-based rainfall data reveal a recent drying trend in central equatorial Africa. *Climatic Change*, *126*(1-2), 263–272. <https://doi.org/10.1007/s10584-014-1217-x>
- Dunning, C. M., Black, E. C., & Allan, R. P. (2016). The onset and cessation of seasonal rainfall over Africa. *Journal of Geophysical Research: Atmospheres*, *121*, 11,405–11,424. <https://doi.org/10.1002/2016JD025428>
- Dyer, E. L. E., Jones, D. B. A., Nusbaumer, J., Li, H., Collins, O., Vettoretti, G., & Noone, D. (2017). Congo Basin precipitation: Assessing seasonality, regional interactions, and sources of moisture. *Journal of Geophysical Research: Atmospheres*, *122*, 6882–6898. <https://doi.org/10.1002/2016JD026240>
- Friedl, M. A., McIver, D. K., Hodges, J. C. F., Zhang, X. Y., Muchoney, D., Strahler, A. H., et al. (2002). Global land cover mapping from MODIS: Algorithms and early results. *Remote Sensing of Environment*, *83*(1-2), 287–302. [https://doi.org/10.1016/S0034-4257\(02\)00078-0](https://doi.org/10.1016/S0034-4257(02)00078-0)
- Friedl, M. A., Sulla-Menashe, D., Tan, B., Schneider, A., Ramankutty, N., Sibley, A., & Huang, X. (2010). MODIS Collection 5 global land cover: Algorithm refinements and characterization of new datasets. *Remote Sensing of Environment*, *114*(1), 168–182. <https://doi.org/10.1016/j.rse.2009.08.016>
- Funk, C., Dettinger, M. D., Michaelsen, J. C., Verdin, J. P., Brown, M. E., Barlow, M., & Hoell, A. (2008). Warming of the Indian Ocean threatens eastern and southern African food security but could be mitigated by agricultural development. *Proceedings of the National Academy of Sciences*, *105*(32), 11,081–11,086. <https://doi.org/10.1073/pnas.0708196105>
- Funk, C., Peterson, P., Landsfeld, M., Pedreros, D., Verdin, J., Shukla, S., et al. (2015). The climate hazards infrared precipitation with stations—A new environmental record for monitoring extremes. *Scientific Data*, *2*(1), 150066. <https://doi.org/10.1038/sdata.2015.66>
- Gelaro, R., McCarty, W., Suárez, M. J., Todling, R., Molod, A., Takacs, L., et al. (2017). The Modern-Era Retrospective Analysis for Research and Applications, Version 2 (MERRA-2). *Journal of Climate*, *30*(14), 5419–5454. DOI: <https://doi.org/10.1175/JCLI-D-16-0758.1>
- Gitau, W., Camberlin, P., Ogallo, L., & Bosire, E. (2018). Trends of intraseasonal descriptors of wet and dry spells over equatorial eastern Africa. *International Journal of Climatology*, *38*(3), 1189–1200. <https://doi.org/10.1002/joc.5234>
- Grist, J. P., & Nicholson, S. E. (2001). A study of the dynamic factors influencing the rainfall variability in the West African Sahel. *Journal of Climate*, *14*(7), 1337–1359. [https://doi.org/10.1175/1520-0442\(2001\)014<1337:ASOTDF>2.0.CO;2](https://doi.org/10.1175/1520-0442(2001)014<1337:ASOTDF>2.0.CO;2)
- Hartter, J., Stamponone, M. D., Ryan, S. J., Kirner, K., Chapman, C. A., & Goldman, A. (2012). Patterns and perceptions of climate change in a biodiversity conservation hotspot. *PLoS ONE*, *7*(2), e32408. <https://doi.org/10.1371/journal.pone.0032408>
- Helsel, D. R., & Hirsch, R. M. (2002). Statistical methods in water resources. In *Hydrologic analysis and interpretation*. Washington, DC: U.S. Geological Survey.
- Hua, W., Zhou, L., Chen, H., Nicholson, S. E., Jiang, Y., & Raghavendra, A. (2018). Understanding the central equatorial African long-term drought using AMIP-type simulations. *Climate Dynamics*, *50*(3–4), 1115–1128. <https://doi.org/10.1007/s00382-017-3665-2>
- Hua, W., Zhou, L., Chen, H., Nicholson, S. E., Raghavendra, A., & Jiang, Y. (2016). Possible causes of the central equatorial African long-term drought. *Environmental Research Letters*, *11*(12), 124002. <https://doi.org/10.1088/1748-9326/11/12/124002>
- Hua, W., Zhou, L., Nicholson, S. E., Chen, H., & Qin, M. (2019). Assessing reanalysis data for understanding rainfall climatology and variability over central equatorial Africa. *Climate Dynamics*, *53*(1–2), 651–669. <https://doi.org/10.1007/s00382-018-04604-0>
- Kalnay, E., Kanamitsu, M., Kistler, R., Collins, W., Deaven, D., Gandin, L., et al. (1996). The NCEP/NCAR 40-year reanalysis project. *Bulletin of the American Meteorological Society*, *77*(3), 437–471. [https://doi.org/10.1175/1520-0477\(1996\)077<0437:TNYRP>2.0.CO;2](https://doi.org/10.1175/1520-0477(1996)077<0437:TNYRP>2.0.CO;2)
- Kizza, M., Rodhe, A., Xu, C. Y., Ntale, H. K., & Hallidin, S. (2009). Temporal rainfall variability in the Lake Victoria Basin in East Africa during the twentieth century. *Theoretical and Applied Climatology*, *98*(1-2), 119–135. <https://doi.org/10.1007/s00704-008-0093-6>
- Levin, N. E., Zipser, E. J., & Cerling, T. E. (2009). Isotopic composition of waters from Ethiopia and Kenya: Insights into moisture sources for eastern Africa. *Journal of Geophysical Research*, *114*, D2306. <https://doi.org/10.1029/2009JD012166>
- Liebmann, B., Bladé, I., Kiladis, G. N., Carvalho, L. M., Senay, G. B., Allured, D., et al. (2012). Seasonality of African precipitation from 1996 to 2009. *Journal of Climate*, *25*(12), 4304–4322. <https://doi.org/10.1175/JCLI-D-11-00157.1>
- Liebmann, B., Hoerling, M. P., Funk, C., Bladé, I., Dole, R. M., Allured, D., et al. (2014). Understanding recent eastern Horn of Africa rainfall variability and change. *Journal of Climate*, *27*(23), 8630–8645. <https://doi.org/10.1175/JCLI-D-13-00714.1>
- Lyon, B., & DeWitt, D. G. (2012). A recent and abrupt decline in the East African long rains. *Geophysical Research Letters*, *39*, L02702. <https://doi.org/10.1029/2011GL050337>

- Maidment, R. I., Allan, R. P., & Black, E. (2015). Recent observed and simulated changes in precipitation over Africa. *Geophysical Research Letters*, *42*, 8155–8164. <https://doi.org/10.1002/2015GL065765>
- Maidment, R. I., Grimes, D., Allan, R. P., Tarnavsky, E., Stringer, M., Hewison, T., et al. (2014). The 30 year TAMSAT African rainfall climatology and time series (TARCAT) data set. *Journal of Geophysical Research: Atmospheres*, *119*, 10,619–10,644. <https://doi.org/10.1002/2014JD021927>
- Maidment, R. I., Grimes, D., Black, E., Tarnavsky, E., Young, M., Greatrex, H., et al. (2017). A new, long-term daily satellite-based rainfall dataset for operational monitoring in Africa. *Scientific Data*, *4*(1), 170063. <https://doi.org/10.1038/sdata.2017.63>
- Monaghan, A. J., MacMillan, K., Moore, S. M., Mead, P. S., Hayden, M. H., & Eisen, R. J. (2012). A regional climatology of West Nile, Uganda, to support human plague modeling. *Journal of Applied Meteorology and Climatology*, *51*(7), 1201–1221.
- Nicholson, S. E. (1996). A review of climate dynamics and climate variability in Eastern Africa. In T. C. Johnson & E. Odada (Eds.), *The limnology, climatology and paleoclimatology of the East African lakes* (pp. 25–56). Boca Raton, FL: CRC Press.
- Nicholson, S. E. (2000). The nature of rainfall variability over Africa on time scales of decades to millenia. *Global and Planetary Change*, *26*(1–3), 137–158.
- Nicholson, S. E. (2014). A detailed look at the recent drought situation in the Greater Horn of Africa. *Journal of Arid Environments*, *103*, 71–79.
- Nicholson, S. E. (2017). Climate and climatic variability of rainfall over eastern Africa. *Reviews of Geophysics*, *55*, 590–635. <https://doi.org/10.1002/2016RG000544>
- Nicholson, S. E. (2018). The ITCZ and the seasonal cycle over equatorial Africa. *Bulletin of the American Meteorological Society*, *99*(2), 337–348.
- Nicholson, S. E., & Dezfuli, A. K. (2013). The relationship of rainfall variability in western equatorial Africa to the tropical oceans and atmospheric circulation. Part I: The boreal spring. *Journal of Climate*, *26*(1), 45–65.
- Nicholson, S. E., & Grist, J. P. (2003). The seasonal evolution of the atmospheric circulation over West Africa and Equatorial Africa. *Journal of Climate*, *16*(7), 1013–1030.
- Nicholson, S. E., Klotter, D., Zhou, L., & Hua, W. (2019). Validation of satellite precipitation estimates over the Congo Basin. *Journal of Hydrometeorology*, *20*(4), 631–656.
- Novella, N. S., & Thiaw, W. M. (2013). African rainfall climatology version 2 for famine early warning systems. *Journal of Applied Meteorology and Climatology*, *52*(3), 588–606.
- Ongoma, V., Chen, H., & Omony, G. W. (2018). Variability of extreme weather events over the equatorial East Africa, a case study of rainfall in Kenya and Uganda. *Theoretical and Applied Climatology*, *131*(1–2), 295–308.
- Otieno, V. O., & Anyah, R. O. (2013). CMIP5 simulated climate conditions of the Greater Horn of Africa (GHA). Part 1: Contemporary climate. *Climate Dynamics*, *41*(7–8), 2081–2097.
- Pohl, B., & Camberlin, P. (2006a). Influence of the Madden–Julian oscillation on East African rainfall. I: Intraseasonal variability and regional dependency. *Quarterly Journal of the Royal Meteorological Society*, *132*(621), 2521–2539.
- Pohl, B., & Camberlin, P. (2006b). Influence of the Madden–Julian oscillation on East African rainfall. II: March–May season extremes and interannual variability. *Quarterly Journal of the Royal Meteorological Society*, *132*(621), 2541–2558.
- Salerno, J., Diem, J. E., Konecky, B. L., & Hartter, J. (2019). Recent intensification of the seasonal rainfall cycle in equatorial Africa revealed by farmer perceptions, satellite-based estimates, and ground-based station measurements. *Climatic Change*, *153*(1–2), 123–139.
- Spracklen, D. V., Arnold, S. R., & Taylor, C. M. (2012). Observations of increased tropical rainfall preceded by air passage over forests. *Nature*, *489*, 282.
- Ssentongo, P., Muwanguzi, A. J., Eden, U., Sauer, T., Bwanga, G., Kateregga, G., et al. (2018). Changes in Ugandan climate rainfall at the village and forest level. *Scientific Reports*, *8*(1), 3551. <https://doi.org/10.1038/s41598-018-21427-5>
- Stein, A. F., Draxler, R. R., Rolph, G. D., Stunder, B. J. B., Cohen, M. D., & Ngan, F. (2015). NOAA's HYSPLIT Atmospheric Transport and Dispersion Modeling System. *Bulletin of the American Meteorological Society*, *96*(12), 2059–2077. <https://doi.org/10.1175/BAMS-D-14-00110.1>
- Stevens, F. R., Gaughan, A. E., Linard, C., & Tatem, A. J. (2015). Disaggregating census data for population mapping using random forests with remotely sensed and ancillary data. *PLoS ONE*, *10*(2), e0107042.
- Todd, M. C., & Washington, R. (2004). Climate variability in central equatorial Africa: Influence from the Atlantic sector. *Geophysical Research Letters*, *31*, L23202. <https://doi.org/10.1029/2004GL020975>
- Washington, R., James, R., Pearce, H., Pokam, W. M., & Moufouma-Okia, W. (2013). Congo Basin rainfall climatology: Can we believe the climate models? *Philosophical Transactions of the Royal Society, B: Biological Sciences*, *368*(1625), 20120296. <https://doi.org/10.1098/rstb.2012.0296>
- Williams, A. P., & Funk, C. (2011). A westward extension of the warm pool leads to a westward extension of the Walker circulation, drying eastern Africa. *Climate Dynamics*, *37*(11–12), 2417–2435.
- Williams, A. P., Funk, C., Michaelsen, J., Rauscher, S. A., Robertson, I., Wils, T. H., et al. (2012). Recent summer precipitation trends in the Greater Horn of Africa and the emerging role of Indian Ocean sea surface temperature. *Climate Dynamics*, *39*(9–10), 2307–2328. <https://doi.org/10.1007/s00382-011-1222-y>
- Yang, W., Seager, R., Cane, M. A., & Lyon, B. (2014). The East African long rains in observations and models. *Journal of Climate*, *27*(19), 7185–7202.
- Yin, X., & Gruber, A. (2010). Validation of the abrupt change in GPCP precipitation in the Congo River Basin. *International Journal of Climatology*, *30*(1), 110–119.
- Zougmore, R. B., Partey, S. T., Ouédraogo, M., Torquebiau, E., & Campbell, B. M. (2018). Facing climate variability in sub-Saharan Africa: Analysis of climate-smart agriculture opportunities to manage climate-related risks. *Cahiers Agricultures*, *27*(3), 34001.